Digital PCR detection of *Mycobacterium tuberculosis* and HIV-1 co-localization in spinal tuberculosis biopsies

Authors:

Robyn Waters[1,2,*], Adrian R Martineau[3], Maritz Laubscher[1], Robert N Dunn[1], Michael Held[1], Melissa-Rose Abrahams[2,4,#], Anna K Coussens[2,5,6,7,#,*]

Author affiliations:

[1]Division of Orthopaedic Surgery, Department of Surgery, Faculty of Health Sciences, University of Cape Town, South Africa.

[2]Wellcome Discovery Platforms in Infection, Institute of Infectious Disease and Molecular Medicine, Faculty of Health Sciences, University of Cape Town, South Africa.

[3]Centre for Immunobiology, Blizard Institute, Faculty of Medicine and Dentistry, Queen Mary University of London.

[4]Division of Medical Virology, Department of Pathology, Institute of Infectious Disease and Molecular Medicine, Faculty of Health Sciences, University of Cape Town, South Africa.

[5]Infection and Global Health Division, Walter and Eliza Hall Institute of Medical Research (WEHI), Parkville, Victoria, Australia.

[6]Division of Medical Microbiology, Department of Pathology, Faculty of Health Sciences, University of Cape Town, South Africa.

19 [7]Department of Medical Biology (WEHI), Faculty of Medicine, Dentistry and Health Sciences,
20 University of Melbourne, Parkville, Victoria, Australia.
21 [#]Equal contribution
22 *Co-corresponding authors
23
24 Contacts:
25 Anna Coussens, Walter and Eliza Hall Institute of Medical Research (WEHI), 1G Royal Parade,
26 Parkville, 3052, Australia; Tel: +61 3 39452699; Email: coussens.a@wehi.edu.au
27 Robyn Waters, Division of Orthopaedic Surgery, University of Cape Town, Anzio Rd,
28 Observatory, 7925, South Africa; Email: robyn.waters@uct.ac.za
29
30
31 Word Count: 3797
32
33 Running Title: *Mtb* & HIV-1 co-location in spinal tissue

ABSTRACT

Background: *Mycobacterium tuberculosis* (*Mtb*) and HIV-1 co-infection in tissues is suggested to favour reciprocal replication, infection and reservoir expansion. Yet, confirmation of this detrimental synergism in diseased tissues is limited.

Methods: In this prospective study of 25 adults investigated for spinal tuberculosis (STB) in South Africa (13 (52%) people living with HIV-1 (PLWH), on antiretroviral treatment) 25 open surgery or CT-guided biopsies were collected and portioned into 93 segments. Extracted DNA was analysed by droplet digital PCR (ddPCR) to detect and quantify *Mtb* complex (MTBC) (*rpoB*, *IS6110*), HIV-1 (*pol*, *gag*) and Human (*RPP30*) gene copies. ddPCR sensitivity for *Mtb* was validated against Xpert-Ultra and culture. Total biopsy and intra-biopsy variation in pathogen DNA abundance, co-detection, and relationships to human cellularity, HIV status, and peripheral viral load (VL) evaluated.

Results: ddPCR detected MTBC DNA in biopsies from 10/10 (100%) culture-confirmed STB, 5/6 (83%) Xpert Ultra-confirmed STB and 4/9 (44%) diagnosed Not STB (all 4 with previous pulmonary TB). Detected MTBC ranged from 8-59,144 *rpoB* copies/biopsy. *RpoB* copies/million human cells were higher in biopsies from PLWH (p=0.0096) and positively correlated with matched-segment HIV-1 *pol* copies/million cells (r=0.40; p=0.0003), but not VL. HIV-1 DNA was detected in all PLWH biopsies, four with undetectable VL. HIV-1 *pol* copies/million cells were higher in segments with MTBC DNA co-detected (p=0.011) and also correlated with VL (r=0.91; p=0.0003).

Conclusions: Reciprocal relationships exists between *Mtb* and HIV-1 abundance in spinal tissue. Findings support investigating TB-HIV co-infected tissue segments to characterise how the immune microenvironment impacts HIV-1/*Mtb* reservoir persistence and/or expansion.

Keywords: STB, ddPCR, diagnostic, *Mtb*, TB-HIV co-infection, HIV reservoir, biopsy, tissue, bone.

60 **INTRODUCTION**

61 In persons living with HIV (PLWH), the presence of HIV-1 co-infection can complicate the
62 diagnosis of tuberculosis (TB), with atypical radiographic findings, reduced sensitivity of
63 diagnostic tools[1], and TB often manifesting in extrapulmonary sites which are difficult to access
64 without invasive procedures.[2] In South Africa, TB-HIV coinfection rates are high, and
65 development of tuberculosis in the spine (STB) is one of the most common EPTB sites in
66 PLWH.[3-6] *Mycobacterium tuberculosis* (*Mtb*) infection of the spine, and associated
67 inflammatory damage to the spinal architecture, is painful and debilitating. Rapid diagnosis on
68 biopsy, using highly sensitive techniques, and prompt initiation of anti-tuberculous treatment,
69 are crucial to reduce morbidity and life-long disability in STB patients.[4,7-11]

70

71 We and others have previously hypothesized that not only may active HIV-1 infection increase
72 *Mtb* replication at co-infection sites precipitating TB development, but that the inflammatory
73 tissue microenvironment at the site of *Mtb* infection may reciprocally increase HIV-1 reservoir
74 size and activation, by driving viral replication and increasing the pool of infection susceptible
75 cells.[12,13] Such a relationship may be particularly evident when TB develops within an HIV-1
76 sanctuary/anatomical reservoir site, given migrating and *Mtb*-specific T cells have increased
77 susceptibility to HIV-1 infection.[14-16] Counter to the often paucibacillary nature of pulmonary
78 TB (PTB) in PLWH, we recently found PLWH on ART had no significant difference in spinal
79 biopsy total *Mtb* abundance, using surrogate measures of time to culture positivity or Xpert
80 MTB/RIF Ultra cycle threshold (Ct), compared to HIV-1 uninfected patients.[17] We also found
81 Xpert MTB/RIF Ultra to have a higher sensitivity than culture in detecting *Mtb* in open surgery
82 and CT-guided biopsies.[17]

83

84 Digital droplet PCR (ddPCR) utility to detect *Mtb* in clinical samples has recently been
85 demonstrated using DNA derived from blood and formalin-fixed and paraffin-embedded
86 (FFPE) samples from EP sites[18-22], although utility for the specific detection of *Mtb* in bone and
87 joint biopsies has yet to be explored. Recent findings in CD34+ stem cells from the whole blood
88 of healthy individuals have implicated the bone marrow as a potential niche for *Mtb* infection,
89 with MTBC DNA more frequently detected by ddPCR in circulating CD34+ cells than CD34-
90 , with increased MTBC DNA detection in PLWH.[22] The bone marrow, as a deep anatomical
91 tissue site, has also been implicated as a viral tissue reservoir that enables the persistence of
92 HIV-1 infection in PLWH on ART[23], although much remains unclear about the mechanisms of
93 this persistence. HIV reservoir quantification is essential for evaluating HIV cure strategies.
94 Multiplexed ddPCR assays also provide the unique opportunity to quantitate the HIV-1
95 reservoir, ensuring sensitive, and specific quantification of viral genomes from multiple HIV-1
96 subtypes including subtype C, which dominates in South Africa and globally, and may thus
97 provide valuable insights into tissue reservoir dynamics following initiation of ART[24-27] and the
98 impact of and on tissue co-localised *Mtb* infection.

99

100 The aim of this study was therefore to optimize and evaluate the utility of ddPCR to detect and
101 accurately quantify *Mtb* and HIV-1 DNA in both open surgery and percutaneous CT-guided
102 needle spinal biopsy tissue, to determine i) if ddPCR is more sensitive than clinically validated
103 tools for *Mtb* detection and quantification in STB biopsies, ii) if HIV-1 proviral DNA can be
104 detected at the site of spinal TB in ART established PLWH, iii) if spinal tissue *Mtb* abundance

105 associates with tissue localised presence and/or abundance of HIV-1, and iv) whether peripheral
106 HIV-1 viral load (VL) is associated with spinal tissue *Mtb* and/or HIV-1 abundance.
107

108 **METHODS**

109 **Study design**

110 This is a sub-study of a prospective, longitudinal, observational cohort previously described.[17]
111 Adults (>18 years) with suspected STB were recruited at Groote Schuur Hospital, a public
112 hospital servicing a population of low socio-economic backgrounds, and low-income
113 households in densely populated vulnerable communities in Cape Town, South Africa, between
114 November 2020 and December 2021. Based on diagnostic results of Xpert MTB/RIF Ultra
115 (GXPU), MGIT TB culture (TBCUL) and histology/histopathology (HIST) from the main
116 study[17], patients were divided into three groups: *Culture-confirmed STB*
117 (TBCUL+GXPU+HIST+), *Xpert Ultra-confirmed STB* (TBCUL-GXPU+HIST+), *Not STB*
118 (TBCUL-GXPU-HIST-, alternate diagnosis Supplementary Table S1). The study was approved
119 by the Human Research Ethics Committee, University of Cape Town (HREC 606/2019).
120 Written informed consent was obtained from all patients.

121 **Data and biopsy collection and processing**

122 Clinical data were collected as previously described[17] and detailed in Supplementary Methods.
123 Spinal biopsy samples were collected via percutaneous CT-guided needle biopsy or open
124 surgery biopsy during mechanical stabilization in theatre, as previously described.[17] Tissues
125 were immediately submerged in DNA/RNA Shield™ (Zymo Research, diluted 1:1 nuclease-

126 free water (Sigma)), maintained at 4°C overnight, and stored at -80°C . Tissue homogenization
127 workflow, DNA extraction and quantification is detailed in Supplementary Methods and
128 Supplementary Figure S1. Briefly, after thawing, larger open biopsies were cut into four equal
129 sized tissue segments measuring approximately 1 cm^2 each homogenized independently for
130 DNA extraction. A fifth sample comprising of combined left-over biopsy homogenate from
131 each of the four segments was also prepared for a separate DNA extraction. Small CT-guided
132 biopsy cores, ranging from 2-7 mm long by 1 mm wide, were used in their entirety as a single
133 sample (Supplementary Figures S2-S3).

134 **ddPCR assays**

135 Three separate ddPCR reactions were prepared for the detection of MTBC (duplex: *rpoB* and
136 *IS6110*), HIV-1 (duplex: *pol* and *gag*) and human housekeeping gene (single-plex: *RPP30*)
137 using a total of 1 µg total DNA each for MTBC and HIV-1 assays and 100 ng for the *RPP30*
138 assay. The inclusion of two *Mtb* targets, *rpoB* and *IS6110*, enhances sensitivity and aids
139 discrimination between high and low mycobacterial loads, characterized by double and single
140 positive results, respectively.[19] The ddPCR method applied for HIV-1 quantification was
141 previously developed for use in blood-derived cells[25], *RPP30* was included to quantify and
142 normalise for human cell count variations across samples. DdPCR assay set-up, accuracy and
143 calculation of MTBC ddPCR limit of detection (LOD) and representative ddPCR amplification
144 plots for samples and no template controls are detailed in Supplementary Materials.

145 All pathogen ddPCR data are presented as either total copies/biopsy, or biopsy segment, and
146 gene copy number per million human cells (copies/million cells), unless otherwise specified.
147 Human cell number was calculated estimating two copies of *RPP30* DNA represents one

148 human nucleated cell (see Supplementary Methods). Normalising to cell number allowed
149 pathogen abundance comparison across varying sample types/sizes. *RPP30* copies/µg were
150 compared between biopsy sample types for assessment of tissue cellularity and the relationship
151 to pathogen abundance. For each sample, MTBC and HIV-1 ddPCR results were considered
152 positive if DNA of either gene was detectable above background signal (i.e.: *rpoB* or *IS6110*
153 and *gag* or *pol*, respectively).

154 **Statistics**

155 Descriptive statistics included median values and interquartile range (IQR) for continuous
156 variables and absolute number (n) and frequency (%) for categorical variables. To assess
157 significant differences between groups, Fisher's exact or Kruskal–Wallis tests and Wilcoxon
158 rank sum tests were used for categorical and continuous variables, respectively. A p-value of
159 <0.05 was considered statistically significant. Statistical analyses were conducted using
160 GraphPad Prism Version 9.3.1. For the duplex *rpoB*/IS*6110* and *gag/pol* assays, the categorical
161 variable was the proportion of patients in whom DNA of either gene was detected, and the
162 continuous variable was the number of copies of *rpoB* and IS*6110*/million cells. Sample size
163 was calculated for the original study [17] and samples used in this study represent a convivence
164 sample, such that a formal power calculation was not performed.

165

166 **RESULTS**

167 **Participant characteristics and total DNA samples for ddPCR derived from spinal**
168 **biopsies**

169 Of the 31 patients enrolled into the parent study, 25 had sufficient additional tissues collected
170 for the ddPCR sub-study, 10 diagnosed *culture-confirmed STB*, 6 *Xpert Ultra-confirmed STB*,
171 and 9 were diagnosed *Not STB* (Figure 1). Patient demographic, clinical and diagnostic
172 characteristics are presented in Table 1 and Supplementary Tables S1-2. Half (8/16) of the
173 patients with confirmed STB, and a third (3/9) of those diagnosed *Not* STB, were males. Those
174 with confirmed SPTB were significantly younger than those without (median age: 40 years
175 *culture-confirmed STB*, 42 years *Xpert-confirmed STB*, 53 years *Not STB*, p=0.02). Of the 25
176 patients, thirteen (52%) were also PLWH (100% ART established), with no difference in HIV
177 status by TB diagnostic group (p=0.22). All reported ART adherence, yet seven (54%) had
178 detectable peripheral VLs (median copies/ml: 446 (IQR: 294-676)), and 4/13 (31%) were
179 virally suppressed (VL unavailable for 2). Seventeen (68%) patients had an open surgery large
180 tissue biopsy specimen collected, whilst eight (32%) underwent percutaneous CT-guided
181 needle biopsy, from which a single core biopsy specimen was collected.

182 From the 25 biopsies, DNA from 93 individual segments was analysed, with open biopsies
183 portioned into five segments (n=17, 85 DNA samples) and CT-guided biopsies analysed as one
184 segment/patient (n=8) (Table 1, Supplementary Figure S1). Open biopsies yielded
185 approximately 100-fold more DNA and human cells (quantified as two *RRP30* copies/cell) than
186 CT-guided biopsies (p<0.0001). There was no difference in the amount of DNA recovered or
187 human cellularity based on open biopsy tissue type, STB diagnostic group or HIV-1 status
188 (Supplementary Figure S4).

189 Of the 93 biopsy segments, 87 (94%) produced valid MTBC ddPCR data (>10,000 droplets),
190 with 62 (67%) samples providing 1 μg of DNA for reactions (Supplementary Figures S5-S6,

191 Table S3). The remaining 31 (33%) samples had less DNA, with a minimum of 46 ng added
192 per reaction and 90 ng the lowest DNA amount that yielded a positive MTBC signal. MTBC
193 assay validation using purified *Mtb* DNA determined detection limits of 2.29 *rpoB* copies/20µl
194 (≈2 bacilli equivalent) and 9.67 IS6110 copies/20µl reaction (Supplementary Figures S5-S6).

195 **ddPCR has high sensitivity to detect MTBC DNA in biopsies from patients with current**
196 **STB and previous PTB**

197 First, to compare MTBC ddPCR performance against Xpert Ultra and TB culture, we combined
198 results from the multiple segments obtained from each biopsy to analyse equivalent total biopsy
199 results. MTBC DNA (*rpoB* or *IS6110*) was detected >LOD in 19/25 (76%) total biopsy samples
200 of suspected STB patients: 10/10 (100%) *culture-confirmed* patients, 5/6 (83%) *Xpert Ultra-*
201 *confirmed* patients and 4/9 (44%) *Not STB* patients (Table 2, individual biopsy results in
202 Supplementary Table S2). The one negative Xpert Ultra-confirmed sample was a CT-guided
203 needle biopsy from a patient initiated on TB treatment before biopsy. The four MTBC DNA
204 patients diagnosed *Not STB* all had previous PTB and one also lymph node (LN) TB; two were
205 *rpoB+IS6110+* and two *rpoB+IS6110-*. Two of these four patients subsequently died (Figure
206 2A, Supplementary Tables S1-S2).

207 MTBC total gene copies/biopsy ranged 8-59,144 for single-copy *rpoB* and 30-1,001,775 for
208 multi-copy *IS6110*, with *rpoB* and *IS6110* total copies/biopsy positively correlated (r=0.8628,
209 p<0.0001, Figure 2B). There was a significant difference in total gene copies/biopsy for both
210 *rpoB* and *IS6110* between those diagnosed as *Not STB* with *culture-confirmed*, but not *Xpert*
211 *Ultra-confirmed* STB patients (Figure 2A). Total copies/biopsy of *rpoB* and *IS6110* were
212 significantly inversely correlated with Xpert Ultra *rpoB* and IS6110 Ct values (r≤-0.597,

213 p<0.017), but ddPCR *rpoB* copies (i.e. bacilli equivalents) were not correlated with culture time
214 to positivity (Figure 2C-D).

215 **MTBC DNA detection and abundance varies between segments of the same biopsy**

216 To investigate the spatial variation in *Mtb* presence and abundance within biopsy tissues, we
217 next compared results between individual biopsy segments (see Figure 3A and Supplementary
218 Figures S2-S3). 45/87 (52%) biopsy segments with valid MTBC results had detectable levels
219 of *IS6110/rpoB*: 29/87 (34%) *rpoB+IS6110+*, 16/87 (18%) single-positive for *rpoB* (15) or
220 *IS6110* (1) (Table 2). Notably, 10/12 *rpoB* single-positive segments came from biopsies that
221 also had double-positive segments, with the single-positive segments generally having ≤20 μg
222 DNA extracted (Figure 3B). The greater detection of *rpoB* single-positives, compared to
223 IS6110, may be explained by the brighter fluorophore used for this probe increasing sensitivity
224 to detect positive droplets above the fluorescence threshold for samples with lower DNA
225 content (Supplementary Figures S7-9). IS6110-negative *Mtb* clinical strains also exist.[28]

226 MTBC DNA was detected in 29/39 (74%) segments from *culture-confirmed* and 11/14 (79%)
227 segments from *Xpert Ultra-confirmed* STB patients. 5/34 (15%) *Not STB* segments had
228 detectable *rpoB*/*IS6110*, 2/34 (6%) *rpoB+IS6110+* (two separate patients) and one *Not STB*
229 patient with previous PTB who died had 2 positive segments (Figure 3B, Table 2).

230 MTBC gene copies/million cells were significantly lower in segments from patients diagnosed
231 *Not STB* compared to STB (p≤0.0002) (Figure 3C). For *culture-confirmed* patients,
232 copies/million cells ranged 10-6,558 for *rpoB* and 55-119,698 for *IS6110*. For *Xpert Ultra-*
233 *confirmed* patients, these were 86-389 and 72-4,045, respectively. In comparison, the five

234 positive biopsy segments from the *Not STB* patients, had 16-61 and 115-154 copies/million
235 cells, respectively (Figure 3C). Combining samples from all patients, *IS6110* and *rpoB*
236 copies/million cells were positively correlated (r=0.814, p<0.0001, Figure 3D). However, when
237 analysing by STB category, correlations remained for *culture-confirmed* (r=0.8265, p<0.0001)
238 and *Not STB* patients (r=0.642, p<0.0001), but not *Xpert Ultra-confirmed* patients (r=0.1264,
239 p=0.6637). Notably, most *Xpert Ultra-confirmed* patients were initiated on TB therapy before
240 biopsy (Supplementary Table 2), thus more extracellular DNA could have been detected.

241 **HIV-1 DNA is detectable in spinal biopsy tissue from PLWH, irrespective of STB**
242 **diagnosis and peripheral viral load**

243 Next, we investigated the ability of ddPCR to detect HIV-1 DNA in spinal biopsy tissues from
244 the 13 PLWH, detecting HIV-1 DNA (*pol*/*gag*) in all 13 biopsies. 34/37 (92%) tissue segments
245 had detectable HIV-1 DNA, 91-100% across STB diagnostic group: 22/37 (60%) were
246 *pol*+*gag*+, 10/37 (27%) were *pol*-*gag*+, and 2/37 (5%) were *pol*+*gag*- (Table 2). Similar to the
247 results for MTBC DNA, double-positive open biopsy segments mostly had >10µg DNA
248 extracted, reflecting high tissue cellularity (Figure 3A and 4A). Of the three patients with HIV-
249 1 DNA detected in less than 5 open biopsy segments, two had lower than detectable (LDL)
250 blood VL, and one had VL 60 copies/ml. In patients who underwent CT-guided biopsies two
251 had LDL VL, 4/6 (67%) were *pol*+*gag*+, 1/6 (17%) *pol*-*gag*+, and 1/6 (17%) *pol*-*gag*+ (Figure
252 4A).

253 Across all PLWH segments, *gag* copies/million cells were significantly higher than *pol*, median
254 (IQR) 254 (75-519) *vs.* 97 (39-305), respectively (p=0.0051), and only modestly correlated
255 (r=0.33, p=0.04) (Figure 4B-C). However, restricting the analysis to *pol*+*gag*+ segments

256 (potentially representing a higher proportion of intact genomes, although not directly
257 measurable by the assay), the positive correlation improved (r=0.7698, p<0.0001).

258 There was also a strong positive correlation between HIV-1 blood VL and the maximum
259 segment *pol* copies/million cells for each patient (r=0.9072, p=0.0003), but not for *gag*
260 (r=0.09305, p=0.7856, Figure 4D). This may support *gag* single positive segments being
261 indicative of defective virus, with *gag* being closer to the 5' end of the HIV-1 genome.

262 **MTBC and HIV-1 abundance are increased in spinal tissue segments where both**
263 **pathogens are detected**

264 To investigate the variation in distribution of both pathogens across biopsy tissues, we first
265 compared the number of open biopsy segments in which each pathogen was detected, finding
266 HIV-1 more widely distributed than *Mtb*: HIV-1 DNA (*gag*/*pol*) detected in 28/31 (90%)
267 segments from PLWH, and MTBC DNA detected in only 35/47 (74%) segments from
268 confirmed STB patients (Figure 3A and 4A). Analysing the impact of HIV-1 co-infection on
269 MTBC (*rpoB/IS6110*) detection in total biopsies, we found no significant difference by patient
270 HIV-1 status (Supplementary Table S4). There was also no difference by HIV-1 status in *rpoB*
271 or *IS6110* total DNA copies/biopsy (Figure 5A), in line with our previous findings based on
272 *Mtb* abundance estimated from culture and Xpert Ultra[17]. However, when analysing biopsy
273 segment results normalised to tissue human cellularity, *rpoB* and *IS6110* copies/million cells
274 were significantly higher in biopsies from PLWH (p≤0.01, Figure 5A).

275 To investigate whether there exists a synergistic interaction between HIV-1 and *Mtb* in spinal
276 tissues we next compared their presence and abundance within 35 biopsy segments from the 13

277 PLWH (STB and Not STB) with valid ddPCR data for both MTBC and HIV-1 DNA. 11/13
278 (92%) patients had MTBC and HIV-1 DNA co-detected in at least one of their open biopsy
279 segments (n=7) or CT-guided biopsy (n=4) (Figure 5B). 20/35 (57%) segments had both MTBC
280 and HIV-1 DNA detected (*rpoB/IS6110* AND *pol*/*gag*), of which 70% (14/20) were
281 *rpoB+IS6110+* and *pol+gag+,* 10% (2/20) *rpoB+IS6110+* and *pol+/gag+,* and 10%
282 *rpoB+IS6110-* and *pol+gag+*.

283 Within individual biopsy segments, MTBC single copy gene *rpoB* copies/million cells were
284 positively correlated with HIV-1 *pol* DNA copies/million cells (r=0.3963, p=0.0003) in the
285 same biopsy segment, but not HIV-1 *gag* copies/million cells (p=0.3595) (Figure 5C).
286 However, maximum biopsy segment *rpoB* copies/million cells and total biopsy MTBC *rpoB*
287 copies were not significantly correlated with blood VL. Therefore indicating *Mtb* abundance at
288 STB tissue sites is positively correlated with local HIV-1 viral genome abundance and not
289 peripheral VL (Figure 5C). Finally, testing the impact of co-localised MTBC presence on tissue
290 segment HIV-1 abundance, we found *pol* copies/million cells were significantly higher in
291 biopsy segments with MTBC DNA co-detected (p=0.0110), whilst there was no significant
292 difference for *gag* copies/million cells (p=0.6002) (Figure 5D).

293

294 **DISCUSSION**

295 Here we report the findings of the first study, to our knowledge, to test for MTBC DNA and
296 HIV-1 DNA in spinal biopsy tissue from patients investigated for STB, living in a setting with
297 a high incidence of both TB and HIV-1 infection[29]. The ddPCR assays successfully detected

298 and quantified MTBC DNA in biopsy tissues from 94% STB confirmed patients and HIV-1
299 DNA in 100% of biopsies from ART-established PLWH, including four peripherally virally
300 suppressed. The ddPCR assay also detected MTBC DNA in biopsies from four patients in which
301 *Mtb* could not be detected by culture or Xpert Ultra, all of whom had a previous PTB diagnosis.
302 Cutting biopsies into segments and normalising pathogen abundance to the localised human
303 cell number enabled investigation of the tissue distribution and co-localised interaction between
304 *Mtb* and HIV-1. Notably, HIV-1 was more widely distributed, being detected in 91% of
305 segments, compared to 74% for *Mtb*. Importantly, whilst maximum tissue localised HIV-1 *pol*
306 copies/million cells strongly correlated with blood VL, MTBC *rpoB* copies/million cells also
307 positively correlated with matched tissue segment HIV-1 *pol* copies/million cells and not blood
308 VL. Thus, our findings support a reciprocal tissue segment localised relationship between *Mtb*
309 and HIV-1 abundance. This finding opens the door for future studies to characterise the
310 immunological difference between co- and mono-infected tissue segments as a means to more
311 precisely characterise the co-infection immune microenvironment and its role in enhancing
312 HIV-1/*Mtb* reservoir persistence/expansion.

313

314 In addition to our creative approach of cutting biopsies into multiple segments to investigate
315 the local microenvironment interaction between *Mtb* and HIV-1 we also normalised pathogen
316 abundance to tissue segment human cell count by measuring copies of *RRP30*, unlike other
317 recent studies which have used ddPCR to investigate MTBC-DNA in blood[22,30]. This enabled
318 identification of a significantly higher abundance of *Mtb* at the site of STB in PLWH, that was
319 not previously found when merely comparing *Mtb* abundance based on total biopsy culture or

320 Xpert values.[17] We had also postulated that with *Mtb* infection, the cellular composition of
321 tissues at the site of disease may be more abundant with recruited and infiltrated cells, however,
322 neither the abundance of *Mtb* infection in the spine nor the abundance of HIV-1 co-infection
323 was associated with biopsy cellularity, although there were trends observed.
324
325 The high sensitivity of ddPCR, enabled low-level detection of MTBC DNA in four patients
326 who were clinically diagnosed STB negative based on culture and Xpert Ultra, all of whom had
327 previous PTB and one also LN TB, two being PLWH. Notably, 68% of the patients with *Mtb*
328 DNA detected in their biopsies by ddPCR had a previous TB episode. *Mtb* may have seeded in
329 the spine via a haematogenous route following pulmonary or LN disease. In the case of the four
330 patients diagnosed *Not STB,* the detected MTBC DNA may have arisen from this previous
331 haematogenous seeding of *Mtb* in the spine that was no longer viable so culture negative, or it
332 represents a misdiagnosis by culture and Xpert Ultra. Positivity was unlikely due to cross-
333 contamination or non-specific amplification, as all 14 biopsy segments from those diagnosed
334 *Not STB* with no previous TB were *rpoB-IS6110-,* as were all negative controls.
335
336 Identifying tissue-based and cellular reservoirs of HIV-1 in ART-treated patients is crucial for
337 finding a cure. Studies have found HIV-1 DNA in bone marrow cells[31,32] and higher than
338 expected levels of HIV proviral DNA in postmortem spinal cord tissue[33]. Our detection of HIV-
339 1 DNA in biopsies from patients with no detectable viral loads in the blood, potentially indicate
340 tissue-specific HIV-1 presence and persistence that is enhanced by *Mtb* tissue presence. As
341 we've previously reviewed[12], the inflammatory state during active *Mtb* infection has the
342 potential to both enhance viral replication, by activating HIV-1 gene transcription from the HIV

343 long terminal repeat promoter region, and creating an expanded cellular niche that is susceptible
344 to HIV-1 infection. HIV-1 establishes latency shortly after infection through integrating into
345 the host genome as a provirus.[34] As ART only inhibits actively replicating virus, it cannot
346 eliminate the virus from latently infected cells, which persist through mechanisms such as
347 homeostatic proliferation[35] and represent a source of viral rebound, if treatment is interrupted.[36]
348
349 Since the HIV reservoir is composed of predominantly replication defective virus, the poor
350 correlation and higher detection of *gag* verses *pol* copies we detected could reflect defective
351 proviral genomes that are hypermutated or have large deletions[37]. Alternatively, this could be
352 due to varying primer sensitivity or off-target amplification. Future studies could include the
353 Intact Proviral DNA Assay (IPDA), a similar ddPCR method with different targets that have
354 increased statistical likelihood of representing intact genomes[24] and combining ddPCR with
355 flow cytometry or single-cell omics to better characterize the HIV-1 reservoir cells.
356
357 The small sample size and single hospital site are limitations of our study, primarily due to the
358 COVID-19 pandemic's impact changing patients' hospital seeking nature. Future work should
359 assess *Mtb* viability through detecting MTBC *16S* mRNA alongside *rpoB* and *IS6110* DNA
360 detection. Our study also highlights the potential improved sensitivity and quantitative accuracy
361 of ddPCR for STB diagnosis, however assessment on larger sample sizes and more diverse
362 patient groups is required to clarify ddPCR's diagnostic performance for STB. While ddPCR's
363 current use is limited by cost and infrastructure[38,39], recent chip-based innovations may
364 overcome these barriers. Further studies should also compare MTBC and HIV-1 DNA detection
365 in peripheral blood compared to disease sites and how these change with treatment, though this

366 would require repeated biopsies. Finally, we did not measure HIV RNA or proteins in tissue
367 biopsies, limiting our ability to determine local HIV replication at MTBC colocalization sites.

368 In conclusion, ddPCR provides highly sensitive detection of *Mtb* in STB biopsies, including in
369 the context of HIV-1 infection, with potential superior sensitivity over Xpert Ultra, and the
370 added benefit of absolute quantification. Through segmenting biopsies into multiple pieces we
371 confirmed a tissue co-localised relationship between *Mtb* and HIV-1 abundance, suggesting
372 both pathogens facilitate expansion of the other in spinal sites of co-infection. This needs to be
373 considered with detection methods and tailored treatment strategies that ensure penetrance into
374 anatomical sites such as the spine. The contribution of the TB microenvironment as both a
375 reservoir and site of HIV reservoir activation requires further investigation.

376

377 **DATA SHARING**

378 Deidentified data from this study will be made available upon request with investigator support,
379 after approval of a proposal, and with a signed data access agreement. For data access, please
380 contact the corresponding author.

381

382 **ACKNOWLEDGMENTS.**

383 We thank Nomsa Yekiso, Nosipho Mncwabe, Dr Qonita Hartley, Dr Chad Centner, Ms Nawaal
384 Adikary and Zeenat Hoosen, orthopaedic surgical teams and our patients for helping,
385 participating and contributing to global evidence. The following reagent was obtained through

386 the NIH HIV Reagent Program, Division of AIDS, NIAID, NIH: HIV-1 Lymphadenopathy-
387 Associated Virus (LAV)-Infected 8E5 Cells, ARP-95, contributed by Dr Thomas Folks. The
388 works was supported by Wellcome (203135Z/16/Z); Academy of Science of SA (ASSAf);
389 ORU, UCT; UCT Merit Award. For the purposes of open access, the authors have applied a
390 CC-BY public copyright to any author-accepted manuscript arising from this submission.

391

392 **DECLARATION OF INTERESTS**

393 The authors have declared that no conflict of interest exists.

394

395 **CONTRIBUTORS**

396 RW collected tissues, performed assays, analysed data and drafted the manuscript. ACK, MRA,
397 MH, and ARM contributed to study design, supported data collection and analysis, and edited
398 the manuscript. RND and ML aided study design, input and sample collection.

399

400

401 **REFERENCES**

402 1. Perkins MD, Cunningham J. Facing the crisis: improving the diagnosis of tuberculosis
403 in the HIV era. *The Journal of infectious diseases* 2007; **196**(Supplement_1): S15-S27.
404 2. Davies P, Pai M. The diagnosis and misdiagnosis of tuberculosis [State of the art series.
405 Tuberculosis. Edited by ID Rusen. Number 1 in the series]. *The International Journal of*
406 *Tuberculosis Lung Disease* 2008; **12**(11): 1226-34.
407 3. Adeyemo S, Sangotola A, Korosteleva O. Modeling transmission dynamics of
408 tuberculosis–HIV co-infection in South Africa. *Epidemiologia* 2023; **4**(4): 408-19.
409 4. Rajasekaran S, Soundararajan DCR, Shetty AP, Kanna RM. Spinal Tuberculosis:
410 Current Concepts. *Global Spine Journal* 2018; **8**(4 Suppl): 96s-108s.
411 5. Govender S, Annamalai K, Kumar K, Govender U. Spinal tuberculosis in HIV positive
412 and negative patients: immunological response and clinical outcome. *International*
413 *orthopaedics* 2000; **24**: 163-6.
414 6. Dunn R, Husien MB. Spinal tuberculosis: review of current management. *The bone &*
415 *joint journal* 2018; **100**(4): 425-31.
416 7. Dunn R. The medical management of spinal tuberculosis. *SA Orthopaedic Journal*
417 2010; **9**: 37-41.
418 8. Held M, Laubscher M, Dix-Peek S, Zar H, Dunn R. Accuracy of GeneXpert PCR
419 Testing in Osteoarticular TB. Orthopaedic Proceedings; 2014: The British Editorial
420 Society of Bone & Joint Surgery; 2014. p. 59-.
421 9. Held M, Laubscher M, Zar HJ, Dunn RN. GeneXpert polymerase chain reaction for
422 spinal tuberculosis: an accurate and rapid diagnostic test. *Bone Joint Journal* 2014; **96-**
423 **b**(10): 1366-9.

424 10. Dunn R, Zondagh I. Spinal tuberculosis: Diagnostic biopsy is mandatory. *SAMJ: South*
425 *African Medical Journal* 2008; **98**(5): 360-2.
426 11. Dunn RN, Ben Husien M. Spinal tuberculosis: review of current management. *Bone*
427 *Joint Journal* 2018; **100-b**(4): 425-31.
428 12. Waters R, Ndengane M, Abrahams M-R, Diedrich CR, Wilkinson RJ, Coussens AK.
429 The *Mtb*-HIV syndemic interaction: why treating *M. tuberculosis* infection may be
430 crucial for HIV-1 eradication. *Future virology* 2020; **15**(02): 101-26.
431 13. He X, Eddy JJ, Jacobson KR, Henderson AJ, Agosto LM. Enhanced human
432 immunodeficiency virus-1 replication in CD4+ T cells derived from individuals with
433 latent mycobacterium tuberculosis infection. *The Journal of infectious diseases* 2020;
434 **222**(9): 1550-60.
435 14. Lopez P, Ajibola O, Pagliuzza A, et al. T cell migration potentiates HIV infection by
436 enhancing viral fusion and integration. *Cell Rep* 2022; **38**(8): 110406.
437 15. Thayil SM, Ho YC, Bollinger RC, et al. *Mycobacterium tuberculosis* complex enhances
438 susceptibility of CD4 T cells to HIV through a TLR2-mediated pathway. *PLoS One*
439 2012; **7**(7): e41093.
440 16. Geldmacher C, Ngwenyama N, Schuetz A, et al. Preferential infection and depletion of
441 *Mycobacterium tuberculosis*-specific CD4 T cells after HIV-1 infection. *J Exp Med*
442 2010; **207**(13): 2869-81.
443 17. Waters R, Laubscher M, Dunn RN, Adikary N, Coussens AK, Held M. Higher
444 sensitivity of Xpert MTB/RIF Ultra over Tuberculosis Culture for the diagnosis of
445 spinal tuberculosis with Open or computed tomography–guided biopsies. *Open Forum*
446 *Infectious Diseases* 2024; **11**(1).

447 18. Cao Z, Wu W, Wei H, et al. Using droplet digital PCR in the detection of
448 *Mycobacterium tuberculosis* DNA in FFPE samples. *International Journal of Infectious*
449 *Diseases* 2020; **99**: 77-83.
450 19. Antonello M, Scutari R, Lauricella C, et al. Rapid Detection and Quantification of
451 *Mycobacterium tuberculosis* DNA in paraffinized samples by droplet digital PCR: a
452 preliminary study. *Frontiers in microbiology* 2021; **12**.
453 20. Yang J, Han X, Liu A, et al. Use of Digital Droplet PCR to Detect *Mycobacterium*
454 *tuberculosis* DNA in Whole Blood-Derived DNA Samples from Patients with
455 Pulmonary and Extrapulmonary Tuberculosis. *Front Cell Infect Microbiol* 2017; **7**: 369.
456 21. Nyaruaba R, Mwaliko C, Kering KK, Wei H. Droplet digital PCR applications in the
457 tuberculosis world. *Tuberculosis (Edinb)* 2019; **117**: 85-92.
458 22. Belay M, Tulu B, Younis S, et al. Detection of *Mycobacterium tuberculosis* complex
459 DNA in CD34-positive peripheral blood mononuclear cells of asymptomatic
460 tuberculosis contacts: an observational study. *The Lancet Microbe* 2021.
461 23. Karris MA, Smith DM. Tissue-specific HIV-1 infection: why it matters. *Future virology*
462 2011; **6**(7): 869-82.
463 24. Buchholtz N, Nühn M, de Jong T, et al. Development of a highly sensitive and specific
464 intact proviral DNA assay for HIV-1 subtype B and C. *Virology Journal* 2024; **21**(1): 1-
465 11.
466 25. Strain MC, Lada SM, Luong T, et al. Highly precise measurement of HIV DNA by
467 droplet digital PCR. *J PloS one* 2013; **8**(4): e55943.
468 26. Bruner KM, Wang Z, Simonetti FR, et al. A quantitative approach for measuring the
469 reservoir of latent HIV-1 proviruses. *Nature* 2019; **566**(7742): 120-5.

470 27. Cassidy NA, Fish CS, Levy CN, et al. HIV reservoir quantification using cross-subtype
471 multiplex ddPCR. *iScience* 2022; **25**(1).
472 28. Zhou L, Ma C, Xiao T, et al. A new single gene differential biomarker for
473 *Mycobacterium tuberculosis* complex and non-tuberculosis mycobacteria. *Frontiers in*
474 *microbiology* 2019; **10**: 1887.
475 29. Mann TN, Davis JH, Walzl G, et al. Candidate biomarkers to distinguish spinal
476 tuberculosis from mechanical back pain in a tuberculosis endemic setting. *Frontiers in*
477 *Immunology* 2021: 4903.
478 30. Armbruster DA, Pry T. Limit of blank, limit of detection and limit of quantitation. *The*
479 *clinical biochemist reviews* 2008; **29**(Suppl 1): S49.
480 31. Carter CC, Onafuwa-Nuga A, McNamara LA, et al. HIV-1 infects multipotent
481 progenitor cells causing cell death and establishing latent cellular reservoirs. *Nature*
482 *medicine* 2010; **16**(4): 446-51.
483 32. Liu Z, Julius P, Kang G, West JT, Wood C. Subtype C HIV-1 reservoirs throughout the
484 body in ART-suppressed individuals. *JCI insight* 2022; **7**(20).
485 33. Riggs PK, Chaillon A, Jiang G, et al. Lessons for Understanding Central Nervous
486 System HIV Reservoirs from the Last Gift Program. *J Current HIV/AIDS Reports* 2022:
487 1-14.
488 34. Chavez L, Calvanese V, Verdin E. HIV latency is established directly and early in both
489 resting and activated primary CD4 T cells. *PLoS pathogens* 2015; **11**(6): e1004955.
490 35. Chomont N, El-Far M, Ancuta P, et al. HIV reservoir size and persistence are driven by
491 T cell survival and homeostatic proliferation. *Nature medicine* 2009; **15**(8): 893-900.

492 36. Price A, Shearman AD, Hamilton TW, et al. 30-day outcome after orthopaedic surgery
493 in patients assessed as negative for COVID-19 at the time of surgery during the peak of
494 the pandemic. 2020; **1**(8): 474-80.
495 37. Bruner KM, Murray AJ, Pollack RA, et al. Defective proviruses rapidly accumulate
496 during acute HIV-1 infection. *Nature medicine* 2016; **22**(9): 1043-9.
497 38. Hindson BJ, Ness KD, Masquelier DA, et al. High-throughput droplet digital PCR
498 system for absolute quantitation of DNA copy number. *Anal Chem* 2011; **83**(22): 8604-
499 10.
500 39. Campomenosi P, Gini E, Noonan DM, et al. A comparison between quantitative PCR
501 and droplet digital PCR technologies for circulating microRNA quantification in human
502 lung cancer. *BMC biotechnology* 2016; **16**(1): 1-10.

503

504 **Table 1. Study patient characteristics, stratified by patient diagnostic group.**

	All Patients (n=25)	TBCUL+ GXPU+HIST+ Culture confirmed STB (n=10)	TBCUL- GXPU+HIST+ Xpert Ultra confirmed STB (n=6)	TBCUL- GXPU-HIST- Not STB (n=9)
Total biopsy segments	93 (100%)	42 (45%)	14 (15%)	37 (40%)
Age, years	48 (36-53)	40 (29-49)	42 (38-44)	53 (49-58)
Male sex	11 (44%)	5 (50%)	3 (50%)	3 (33%)
HIV-1 positive patients	13 (52%)	6 (60%)	4 (67%)	3 (33%)
Undetectable HIV-1 VL	4/11[A] (36%)	2/5[A] (40%)	1/3[A] (33%)	1 (33%)
Detected HIV-1 plasma VL	446 (294-791)	372 (292-391)	1137 and 49959	60 and 676
Previous TB history	14 (56%)	5 (50%)	4 (67%)	5 (56%)
TB therapy initiated before biopsy	9 (28%)	3 (30%)	5 (83%)	1 (11%)
TB culture positive	10 (40%)	10 (100%)	0 (0%)	0 (0%)
Xpert MTB/RIF Ultra +	16 (64%)	10 (100%)	6 (100%)	0 (0%)
Histopathology +	12/19[B] (63%)	7/7 (100%)	5/5 (100%)	0/7 (0%)
AFB +	2/18[C] (11%)	2/8 (25%)	0/5 (0%)	0/5 (0%)
Open surgery biopsy	17 (68%)	8 (80%)	2 (33%)	7 (78%)
CT-guided needle biopsy	8 (32%)	2 (20%)	4 (67%)	2 (22%)

505 Data are proportion (n) and (%) or median (IQR). [A]n=2 unavailable viral load (VL) results (1 culture confirmed
506 and 1 Xpert Ultra confirmed); n=4 lower than detectable limit (LDL); [B]No histology report available in n=6
507 patient (3 culture confirmed, 1 Xpert Ultra confirmed, 2 Not STB); [C]No Ziehl-Neelsen staining report for acid
508 fast bacilli (AFB) available in n=7 patients (2 culture confirmed, 1 Xpert Ultra confirmed, 4 Not STB);. +:
509 positive; -: negative; CT: Computed tomography; CUL culture; GXPU: Xpert MTB/RIF Ultra; HIST: histology;
510 TB: Tuberculosis.

511
512

513 **Table S2. Total biopsy and biopsy segment ddPCR detection of MTBC and HIV-1 DNA, stratified by STB**
514 **diagnostic group.**

	TBCUL+GXPU+ HIST+ Culture Confirmed STB	TBCUL-GXPU+ HIST+ Xpert Ultra Confirmed STB	TBCUL-GXPU- HIST- Not STB	All Patients
Total Biopsy, all patients	**n=10**	**n=6**	**n=9***	**n=25**
MTBC DNA ddPCR+	10 (100%)	5 (83%)	4 (44%)	19 (76%)
rpoB+IS6110+	9 (90%)	5 (83%)	2 (22%)	16 (64%)
rpoB+IS6110-	1 (10%)	0 (0%)	2 (22%)	3 (12%)
rpoB-IS6110+	0 (0%)	0 (0%)	0 (0%)	0 (0%)
rpoB-IS6110-	0 (0%)	1 (17%)[#]	5 (56%)	6 (24%)
Biopsy segments, all patients	**n=39**	**n=14**	**n=34**	**n=87**
MTBC DNA ddPCR+	29 (74%)	11 (79%)	5 (15%)	45 (52%)
rpoB+IS6110+	19 (49%)	8 (58%)	2 (6%)	29 (34%)
rpoB+IS6110-	9 (23%)	3 (21%)	3 (9%)	15 (17%)
rpoB-IS6110+	1 (3%)	0 (0%)	0 (0%)	1 (1%)
rpoB-IS6110-	10 (25%)	3 (21%)	29 (85%)	42 (48%)
Total biopsy, HIV+ patients	**n=6**	**n=4[^]**	**n=3**	**n=13**
HIV-1 DNA ddPCR+	6 (100%)	4 (100%)	3 (100%)	13 (100%)
pol+gag+	6 (100%)	3 (75%)	2 (67%)	11 (84%)
pol+gag-	0 (0%)	1 (25%)	0 (0%)	1 (8%)
pol-gag+	0 (0%)	0 (0%)	1 (33%)	1 (8%)
pol-gag-	0 (0%)	0 (0%)	0 (0%)	0 (0%)
Biopsy segments, HIV+ patients	**n=22**	**n=4[^]**	**n=11**	**n=37**
HIV-1 DNA ddPCR+	20 (91%)	4 (100%)	10 (91%)	34 (92%)
pol+gag+	13 (59%)	3 (75%)	6 (55%)	22 (59%)
pol+gag-	1 (5%)	1 (25%)	0 (0%)	2 (5%)
pol-gag+	6 (27%)	0 (0%)	4 (36%)	10 (27%)
pol-gag-	2 (9%)	0 (0%)	1 (9%)	3 (8%)

515 Data are presented as n (%) per diagnostic group. GXPU: Xpert MTB/RIF Ultra, HIST: Histology, TBCUL:
516 MGIT TB culture. 87/93 biopsy segments had valid MTBC ddPCR data points and 37/41 HIV+ biopsy segments
517 had valid HIV-1 ddPCR >10,000 droplets.
518 *5/9 diagnosed *Not STB* had previous pulmonary TB, 4/5 of these were MTBC DNA ddPCR+.
519 [#]Sample was CT-guided biopsy and patient initiated on TB treatment before biopsy.
520 [^]All four CT-guided biopsies.
521
522

523

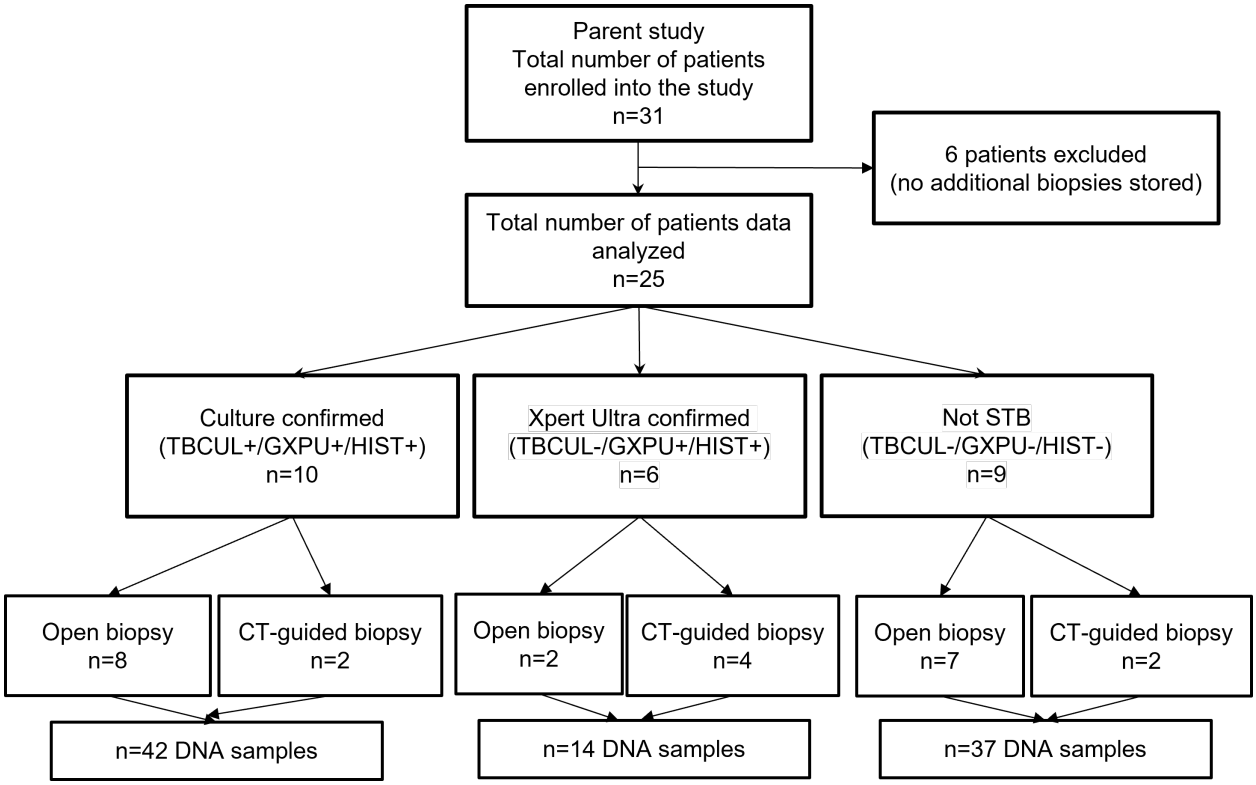

524

525

526 **Figure 1. Flow diagram of study patients including diagnostic, surgical, and ddPCR sample categories**.
527 *GXPU: Xpert MTB/RIF Ultra; TBCUL: MGIT TB culture; HIST: histology including histopathology and Ziehl-*
528 *Neelsen stain for acid fast bacilli.*
529

530
531

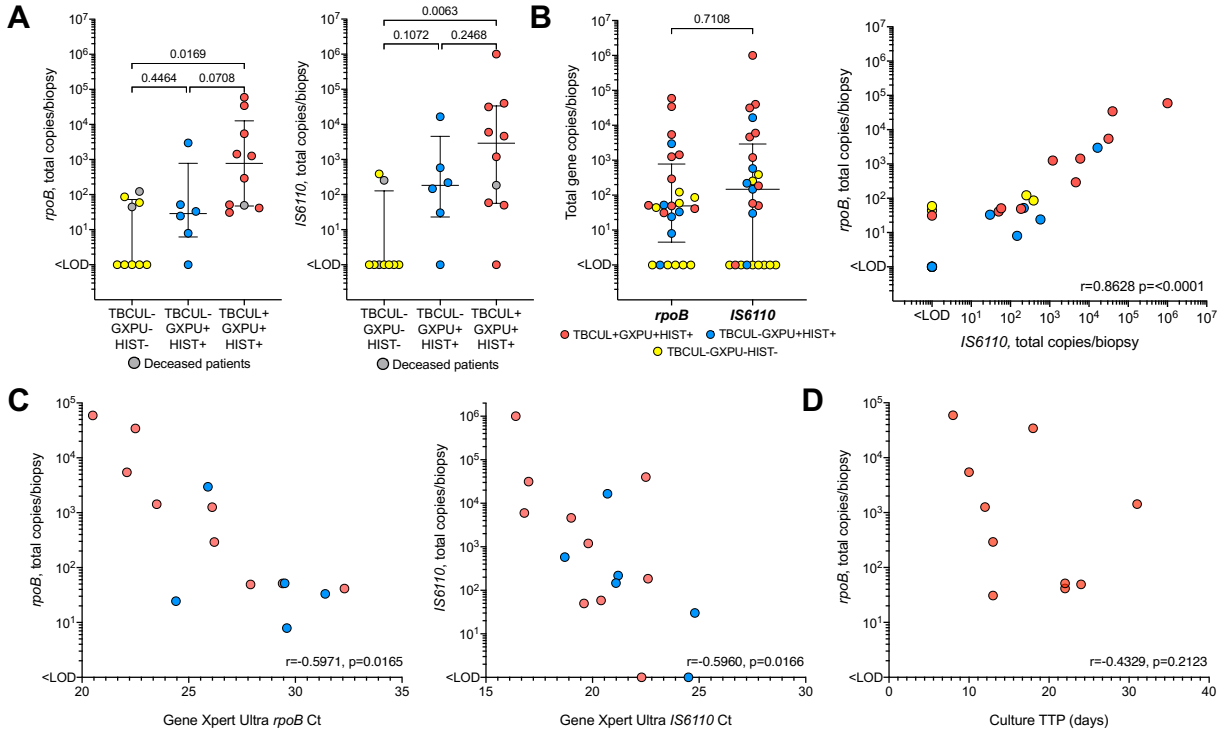

Figure 2. Total biopsy ddPCR MTBC gene copies from adult patients investigated for STB, undergoing either percutaneous CT-guided needle biopsy or open biopsy in theatre. A) Total *rpoB* and *IS6110* copies per biopsy, stratified by STB diagnostic group. Grey dots represent deceased patients who passed away after diagnosis. **B**) Total *rpoB* and *IS6110* copies, per total biopsy, for all patients combined. Data plotted as median + IQR and the Spearman's correlation between *IS6110* and *rpoB* total copies per biopsy. **C**) Total *rpoB* ddPCR copies and *IS6110* copies per biopsy, correlated with Gene Xpert MTB/RIF Ultra (GXPU) *rpoB* and *IS6110* Ct values, respectively, colored by STB diagnostic group in A-B. One GXPU positive did not have *rpoB* Ct values. **D**) Total *rpoB* copies/biopsy correlated with MGIT TB culture (TBCUL) time to positivity (TTP). Dots represent combined biopsy segment results for each patient. (A-B) Kruskal-Wallis test with Benjamini, Krieger and Yekutieli FDR (q-value) and (B-D) Spearman correlation coefficients and p values calculated using Spearman's test. HIST: Histology, LOD: Limit of detection.

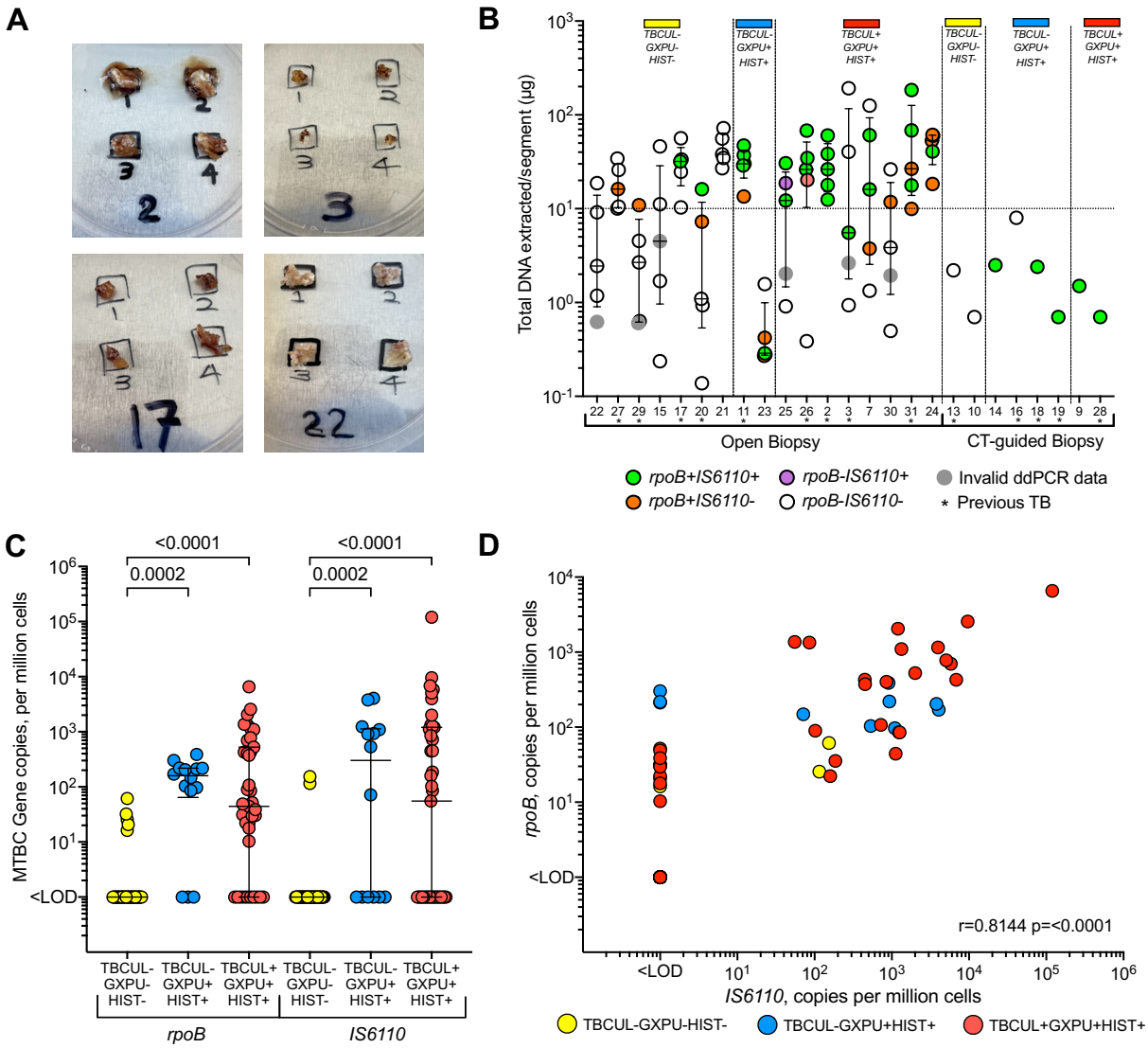

Figure 3. MTBC *rpoB* and *IS6110* copies detected by ddPCR. **A)** Representative images of segmented open spinal biopsies with diseased soft (##2,3,17) or hard bone (#22), B) MTBC DNA detection in total DNA extracted per segment of open biopsy patients, or some the entire CT-guided needle biopsy core, stratified by STB diagnostic group**.** Individual dots represent total DNA extracted per biopsy segment (n=5 open biopsy, n=1 CT-guided biopsy). Double positives (*rpoB+IS6110+*, green dots; no *rpoB* or *IS6110* detected (*rpoB-IS6110-,* white dots with black border); single positives (*rpoB+IS6110-,* orange dots; single positives (*rpoB-IS6110+,* purple dots). X-axis labelled with patient ID. **C**) Gene copies in biopsy segments, stratified by STB diagnostic grouping**.** *rpoB* and *IS6110* copy numbers per million human cells for n=87 segments with valid ddPCR data. <LOD was 'undetectable'. Kruskal-Wallis Test with Benjamini, Krieger and Yekutieli FDR (q-value). Lines show median values with IQR. **D)** *IS6110* versus *rpoB* copies/million cells for the 87 biopsy segments with valid ddPCR data. X and Y axes are log10. Spearman correlation coefficients and p values were calculated using Spearman's test. GXPU: Xpert MTB/RIF Ultra, HIST: Histology, LOD: Limit of detection, TBCUL: MGIT TB culture.

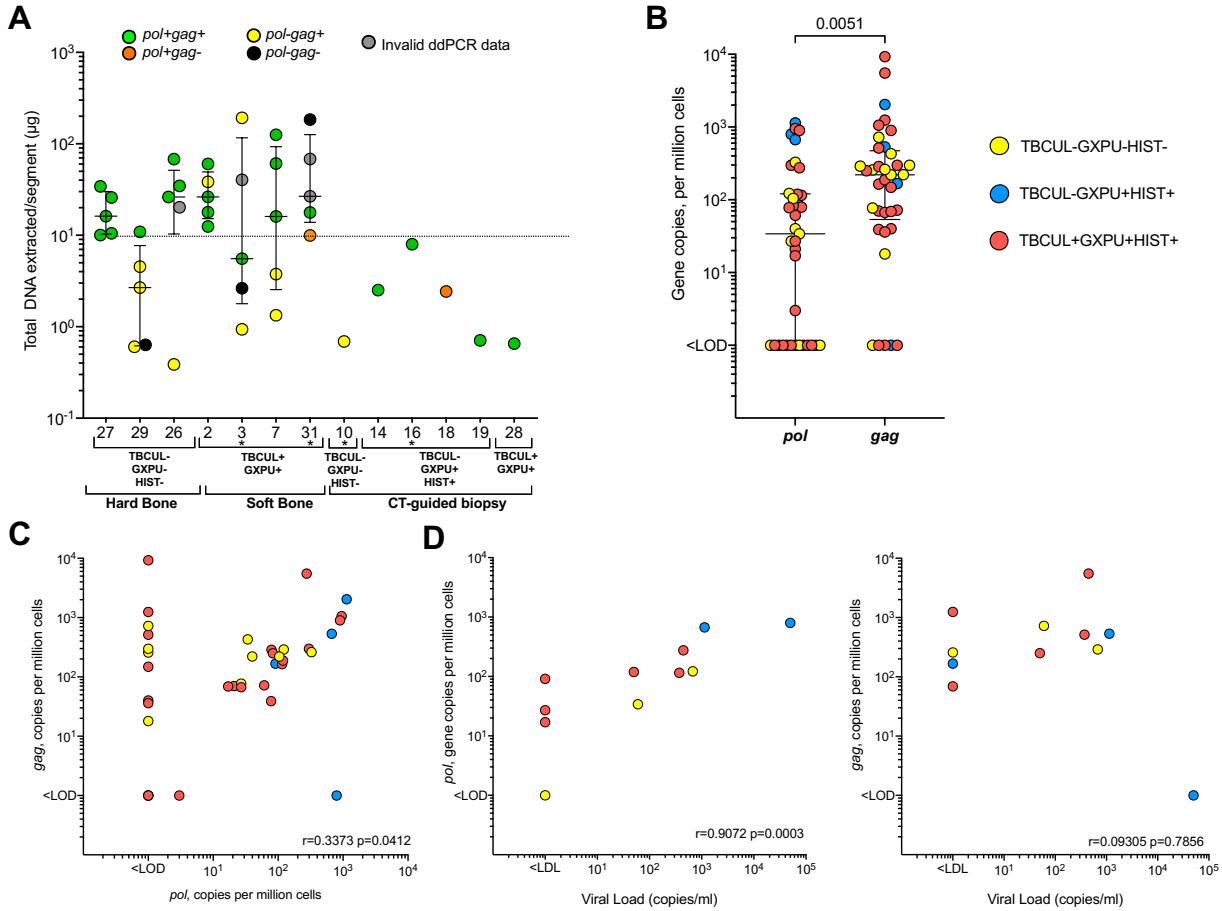

Figure 4. Detection of HIV-1 DNA in spinal biopsy tissue from PLWH and the relationship to blood viral load. A) HIV-1 DNA detection in total DNA extracted per segment of open biopsy from PLWH, stratified by STB diagnostic group and type of tissue extracted during surgery. Individual dots represent total DNA extracted per five biopsy segments from each patient. X axis is patient ID. *Pol* and *gag*: HIV-1 genes. Invalid ddPCR: samples with droplet counts <10 000, no detection by software. * on patient ID indicates those with blood viral load lower than detectable levels. **B**) Detection and **C**) correlation of HIV-1 *pol* and *gag* gene copies per million cells in DNA from biopsy tissues of adult suspected spinal tuberculosis patients. **D**) Correlation between spinal biopsy maximum detected *pol* or *gag*, copies per million cells across tested biopsy segments and plasma HIV-1 viral load. Correlation coefficients and p-values were calculated with Spearman's test. n=2 patients had unknown viral loads and were excluded from D and E analysis. *GXPU: Xpert MTB/RIF Ultra; HIST: Histology; TBCUL: MGIT TB culture.*

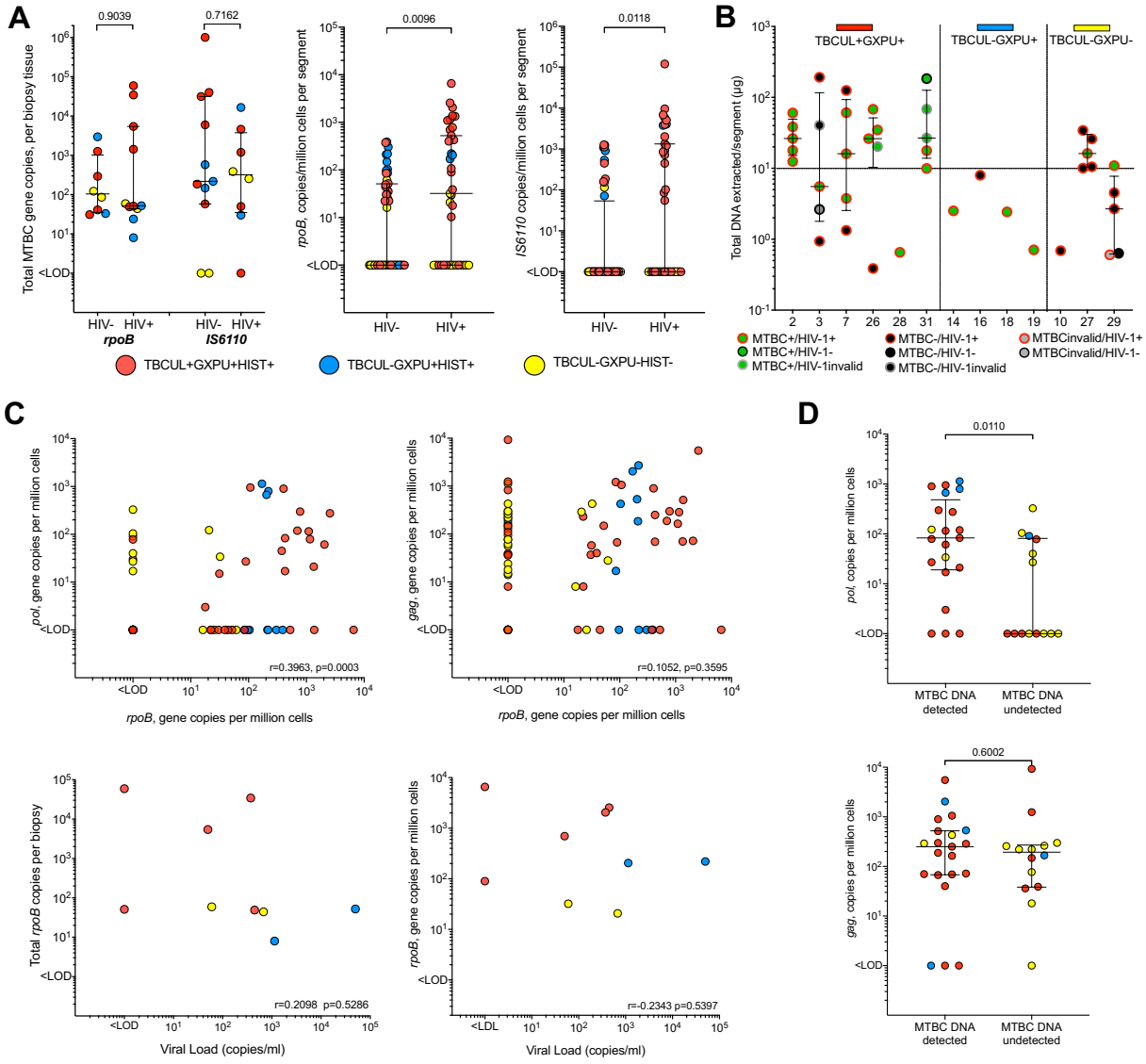

Figure 5. Relationship between MTBC DNA abundance and HIV-1-status, gene copies, and co-detection of MTBC DNA in spinal TB biopsy tissues. A) Total MTBC *rpoB* and *IS6110* copies/biopsy tissue, by HIV status, and *rpoB* and *IS6110* copies/million cells per biopsy segment, by HIV status. (**B)** Detection of both MTBC and HIV-1 DNA in biopsy segments from open and CT-guided biopsy from PLWH, stratified by STB diagnostic group. Individual dots represent total DNA extracted per biopsy segment for either open (n=5/patient) or CT-guided biopsies (n=1/patient). MTBC+ = detection of *rpoB* or *IS6110* and HIV-1+ = detection of *pol or gag.* X axis is MUTI patient ID. MUTI016 was on empiric anti-tuberculous therapy at the time for concurrent pulmonary TB with undetectable MTBC DNA yet detectable HIV-1 DNA. (**C**) Correlation between HIV-1 *pol* or *gag* copies/million cells with *rpoB* copies/million cells in each biopsy segment and correlation between patient HIV-1 VL in the blood and spinal biopsy total detected *rpoB* copies or maximum biopsy segment *rpoB* copies/million cells. (**D**) HIV-1 gene copies/million cells for *pol* and *gag* in biopsy samples stratified by whether MTBC DNA (either *rpoB or IS6110*) was detected by ddPCR. P values were calculated with Mann-Whitney tests (A,D). Correlation coefficients and p-values were calculated with Spearman's test (C)). Lines show median values with interquartile range (IQR). Dots in all graphs coloured by STB diagnostic group, as per (A). *GXPU: Xpert MTB/RIF Ultra; MTBC: Mycobacterium tuberculosis complex; TBCUL: MGIT TB culture. LOD: limit of detection.*